ELSEVIER

Quinazoline derivatives as MC-I inhibitors: Evaluation of myocardial uptake using Positron Emission Tomography in rat and non-human primate

Ajay Purohit,[a,*] Richard Benetti,[b] Megan Hayes,[a] Mary Guaraldi,[a] Mikhail Kagan,[a] Padmaja Yalamanchilli,[a] Fran Su,[c] Michael Azure,[a] Mahesh Mistry,[a] Ming Yu,[a] Simon Robinson,[a] Douglas D. Dischino[d] and David Casebier[a]

[a]Bristol-Myers Squibb Medical Imaging, 331 Treble Cove Road, N. Billerica, MA 01860, USA
[b]Boston University Medical School, 715 Albany Street, Boston, MA 02118, USA
[c]New York University Stern School Of Business, 44 West Fourth Street, New York, NY 10012, USA
[d]Bristol-Myers Squibb, Pharmaceutical Research Institute, 5 Research Parkway, Wallingford, CT, USA

Abstract—Several quinazoline derivatives were made as mitochondrial complex 1 inhibitors. Compound **4** showed an IC_{50} of 11.3 nM and was the most potent compound of this series. The ^{18}F analog of **4**, $[^{18}F]$ **4**, was injected in the rat and showed high and rapid heart uptake, fast liver clearance, and low blood uptake. Images obtained using a μPET showed clear delineation of the myocardium in normal rats and perfusion deficit in ischemic rats. In the non-human primate, $[^{18}F]$ **4** showed rapid uptake and clearance from the myocardium and high liver uptake.
© 2007 Elsevier Ltd. All rights reserved.

Coronary artery disease (CAD) afflicts an estimated 13 million Americans making it the most common form of heart disease. CAD and its complications, like arrhythmia, angina pectoris, and myocardial infarction, are the leading causes of death in the United States. A common way of detecting CAD is to image myocardial blood flow using either ^{99m}Tc-sestamibi (Cardiolite®), Thallium (^{201}Tl) or tetrofosmin.[1] Cardiolite®, the current gold standard for imaging myocardial blood flow, is a ^{99m}Tc based agent and has gained widespread acceptance due to the high quality planar and computed tomographic images that are accompanied by sharper delineation of myocardial walls and less granularity compared to ^{201}Tl. However there exist inherent drawbacks to SPECT based imaging, which include: (1) limited spatial and temporal resolution; (2) lack of accurate attenuation correction; (3) inadequate partial volume effect correction; (4) inability to quantify blood flow in ml/g/min.

Positron Emission Tomography (PET) together with appropriate tracer kinetic models has the ability to quantify myocardial blood flow in absolute units in the human heart and therefore permits evaluation of coronary function. With this knowledge we initiated a program to develop a PET based agent for imaging myocardial perfusion. Myocardial tissue contains approximately 30% mitochondria by weight.[2] Four mitochondrial complexes (MC I-IV) comprise the electron transport chain (ETC) and are found in the inner membranes of the mitochondria. The first in this chain is ubiquinone oxidoreductase, termed mitochondrial complex 1 (MC-I). The MC-I complex is a membrane-bound protein complex of 43 dissimilar subunits and is the entry point for electrons, in the form of $NADH + H^+$, derived from glycolysis, the tricarboxylic acid cycle, and fatty acid oxidation and channels these electrons into the electron transport chain. This chain terminates with the reduction of oxygen to water and synthesis of ATP via oxidative phosphorylation. The MC-I complex has been the subject of extensive investigation. One study assessed defects in mitochondrial function to image certain nervous system disorders like Parkinson's and Huntington's disease.[3] It has also been

evaluated as a potential target for imaging myocardial perfusion[4] using ^{125}I SPECT.
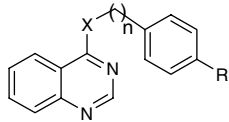
Rotenone is known to be the classical MC-I inhibitor and a plethora of synthetic and naturally occurring inhibitors for this complex are known.[5] Rotenone is a natural product present in both the cube resin (Lonchocarpa sp.) and derris root (Derris *elliptica*) and is a known and widely used insecticide, aracaricide or a piscicide. Recent reports have shown that rotenone derivatives labeled with ^{125}I and ^{18}F have excellent cardiac uptake, good background/organ ratios, and good kinetics.[3d,e] We therefore stated looking toward compounds that had similar affinity for the target of rotenone, and chose Fenazaquin (entry 1, Table 1) as a lead structure. Fenazaquin, **1**, is a highly potent inhibitor of MC-I function[6] (IC$_{50}$ = 4 nM), has been widely studied, and possesses an uncomplicated structure. Fenazaquin has also been shown to share a common binding domain in the MC-I complex with rotenone.[7,8] In this paper, we wish to describe synthesis of 4-substituted quinazo-

lines as MC-I inhibitors and our initial PET imaging studies for assessing myocardial blood flow in rats (normal and ischemic) and monkeys.

Most synthetic inhibitors of MC-I have a common topology. They consist of a headpiece, usually an aromatic heterocycle, a linking moiety, usually a heteroalkyl chain, and a side chain, typically an aromatic ring with an alkyl group in the *para* position to the linking group. Prior research in this area indicated flexibility in the SAR of fenazaquin side chain[9–12] rather than the quinazoline core itself.[13] Therefore, we first sought to replace the tertiary butyl group present on the phenyl ring with a normal butyl group. This would enable us to introduce a fluorine (1° or 2°) by a S$_n$2 reaction and at the same time maintain the hydrophobicity of the side chain. The activity of the *n*-butyl analog of fenazaquin, compound **2**, though nine times less than fenazaquin pointed to the fact that less bulky aliphatic groups could be used to modulate the activity. Replacement of a hydrogen and/or hydroxyl groups with fluoride is a well-established strategy in drug development and often leads to increase in potency.[14] Keeping this in mind we sought to make two fluorobutyl analogs: (a) the 4-fluorobutyl analog, **4**, and (b) the benzylic analog, **6**. If active both these compounds could then be converted to their ^{18}F analogs. As expected both **4** and **6** were more potent (IC$_{50}$: 11.1 and 19.3 nM, respectively) than the parent compound **2**. We however did not pursue compound **6** due to concerns regarding the potential for hepatic (cytochrome P$_{450}$) oxidation and defluorination.[15] At this stage we wanted to assess the viability of quinazolines as potential imaging agents and decided to make the ^{18}F version of **4**. Compound [^{18}F] **4** was therefore synthesized via the alcohol **3** and through the corresponding *p*-toluenesulfonate ester **11** (Scheme 1) and imaged in the rat, rabbit, and the non-human primate.

We also wanted to explore the effect of other modifications on activity and therefore synthesized compounds **7**, **8**, and **9**. Compounds **7** and **8** which contain a meth-
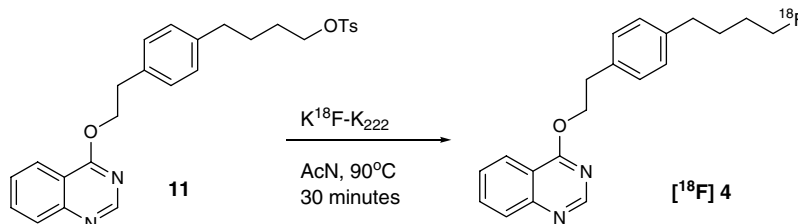
Table 1. Structure–activity table for various fenazaquin derivatives

Entry	R	n	X	MC-I inhibition[16] IC$_{50}$ (nM)
1 (Fenazaquin)	–C(CH$_3$)$_3$	2	O	4
2	–CH$_2$(CH$_2$)$_2$CH$_3$	2	O	37.5
3	–CH$_2$(CH$_2$)$_2$CH$_2$OH	2	O	22.4
4	–CH$_2$(CH$_2$)$_3$CH$_2$F	2	O	11.3
5	–CH(OH)(CH$_2$)$_2$CH$_3$	2	O	21.7
6	–CH(F)(CH$_2$)$_2$CH$_3$	2	O	19.3
7	–CH$_2$(CH$_2$)$_2$CH$_3$	1	O	1000
8	–CH$_2$(CH$_2$)$_2$CH$_2$OH	1	O	414
9	–C(CH$_3$)$_3$	1	NH	241
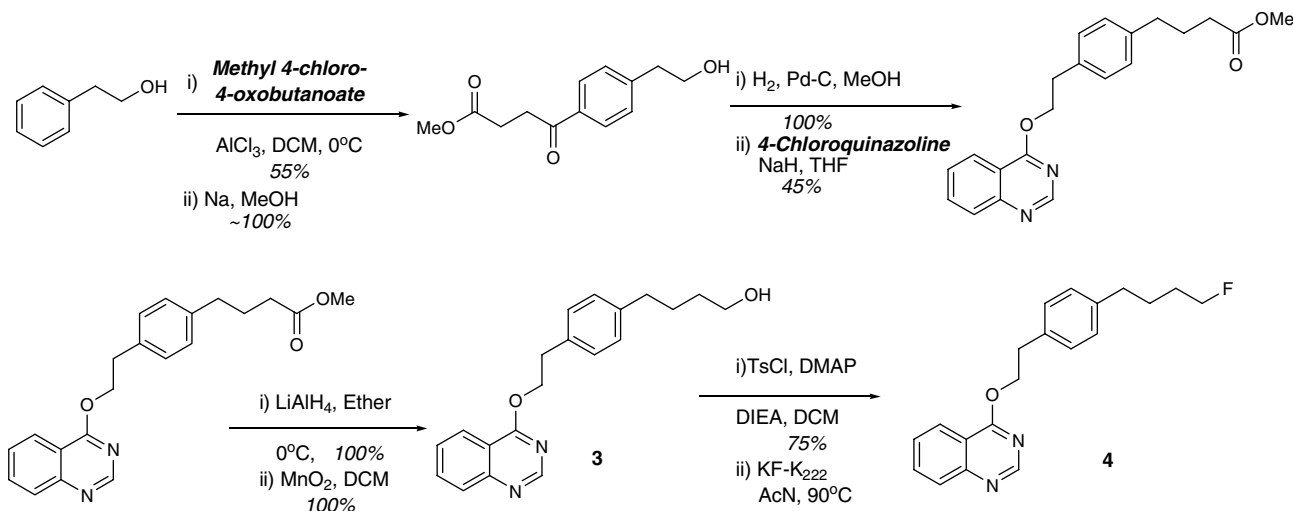
Scheme 1. Synthetic route for **3**.

Scheme 2. Radiosynthesis of [^{18}F] **4**.

ylene linker (benzylic analogs) were made with this purpose. Clearly the activity is strongly dependent on the linker length with **7** and **8** being 26- and 11-fold less active than **2**, respectively. It is worth noting that **3** and **8** both of which contain a hydroxyl in the 4 position are more active than **2** and **7**. This can be attributed to the hydroxyl group participating in hydrogen bond interactions. The benzyl amino analog **9** to our surprise was found to be more active than the benzyl oxy analogs **7** and **8** and this could be attributed to either the hydrogen bond *donating* ability of the amine or to the conformational change brought about by the amine.

It is known that certain lipophilic cationic species can cross the mitochondrial membrane.[17–19] Thus a discreet methyl quinazolinium iodide[20,21] was made based on this premise.[22] This compound however showed poor activity in the MC-I assay (IC$_{50}$ > 4000 nM) and was therefore not pursued further.

Only the synthetic route for compound **4** is shown in Scheme 1 and MC-I inhibition activities for all compounds are shown in Table 1.

Radiochemistry, bio-distribution, and μPET imaging.

Radiochemistry. All glassware was silanized to preclude adhesion of the material to the vessel walls and optimize transfers. Compound [^{18}F] **4** was synthesized by treating **11** with [^{18}F] KF in the presence of kryptofix (K$_{222}$)[23] in an acetonitrile solution at 90 °C for 30 min. After cooling at 45 °C the contents of the flask were diluted with water, loaded onto a Oassis™ and HLB-C18 Sep-Pak column. The cartridge was washed with water (2 × 5 ml for the removal of salts and highly polar by-products). The desired material was then eluted from the cartridge with 90% acetonitrile/10% water. The purified compounds were analyzed via HPLC using a Zorbax C-18 column (250 × 4.6 mm 5μ particle size, 100 Å pore size). Concentration of the solution in vacuo (either by rotary evaporation or vacuum/air bleed) afforded material which was reconstituted in a minimal (ca. 100 μl) volume of ethanol, and diluted to dose volume with sterile water. The radiochemical purity of a typical sample was >95% and the typical radiochemical yield based on ^{18}F (corrected for decay) was 15% (Scheme 2).

Tissue biodistribution of [^{18}F] 4 in rats. Tissue biodistribution of [^{18}F] **4** was examined in sodium pentobarbital (50 mg/kg) anesthetized Sprague–Dawley (SD) rats. Post-anesthesia, a cannula was inserted into the left

femoral vein of rats and [^{18}F] **4** (ca. 15 μCi per rat) was injected intravenously. At 30 and 120 min post-injection (mpi) the rats were sacrificed and tissue samples were collected, weighed, and counted for radioactivity. The biodistribution of [^{18}F] **4** was expressed as % injected dose per gram of tissue (% ID/g, Table 2). As shown in Table 2, [^{18}F] **4** preferentially accumulated in the myocardium of rats. The myocardial uptake was 3.2 ± 9.15% ID/g at 30 mpi and the activity in the heart remained constant over 120 min (2.5 ± 0.18% ID/g). In contrast, the background lung and liver uptake were low and the blood clearance was also rapid. Uptake in the femur increased over time (0.65% vs 0.19% ID/g at 120 and 30 mpi, respectively).

As is shown in Table 3, the ratios of uptake in the heart vs. three other organs (lung, liver and femur) were also very high leading to clear delineation of the myocardium with virtually no background interference.

μPET imaging. In vivo imaging studies were performed in the micro-PET Focus-220. The rat was anesthetized with sodium pentobarbital (50 mg/kg) and 1 mCi [^{18}F] **4** was administered intravenously via the femoral vein and images were acquired after 5, 30, 60, and 120 min. Compound [^{18}F] **4** clearly showed rapid uptake in the hearts of rats and the non-human primate but retention was species dependent. Compound [^{18}F] **4** is retained in the rat myocardium but washed out from that of the non-human primate after an hour. The myocardial out-

Table 2. Tissue biodistribution of [^{18}F] **4** in rats expressed as mean ± SD

Organ	30 min (*n* = 3)	120 min (*n* = 5)
Heart	3.22 ± 0.15	2.50 ± 0.18
Blood	0.08 ± 0.01	0.06 ± 0.00
Lung	0.28 ± 0.01	0.11 ± 0.01
Liver	1.29 ± 0.05	0.44 ± 0.07
Spleen	0.19 ± 0.01	0.07 ± 0.01
Kidney	1.99 ± 0.21	0.68 ± 0.06
Urine	0.50 ± 0.24	4.44 ± 1.46
Muscle	0.08 ± 0.00	0.12 ± 0.01
Femur	0.19 ± 0.03	0.65 ± 0.18

Table 3. Heart to organ ratios in the rat for [^{18}F] **4**

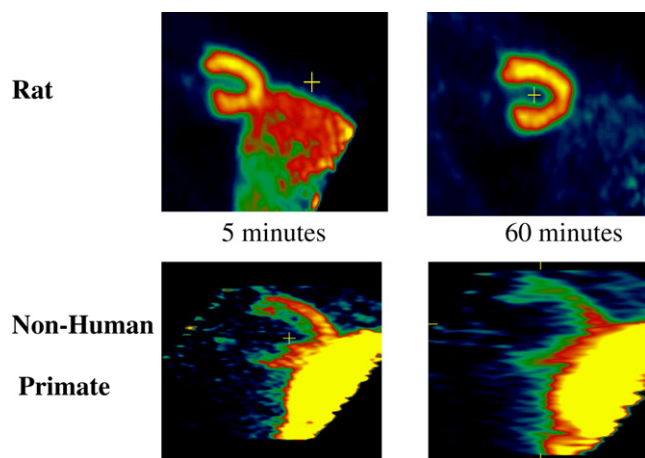|	Heart/lung	Heart/liver	Heart/femur
30 min	11.3	23	16.8
60 min	2.5	5.7	3.6

Figure 1. μPET imaging of the rat and non-human primate.

line was clear and defined in the rat, whereas that of the non-human primate was diffuse. This was due primarily to rapid liver clearance in the rat with very little activity present after 15 min (images not shown). The opposite was true in the case of the non-human primate. The liver retained most of its initial activity making the heart difficult to visualize, particularly the left ventricular inferior wall (Fig. 1).

In summary, we have synthesized a series of quinazolines that inhibit MC-I and labeled an exemplary compound with ^{18}F for myocardial perfusion imaging. Based on the excellent uptake and images in the rat this agent was imaged in the primate but showed high liver retention and rapid washout from the myocardium. The bio-distribution was highly species dependent.

References and notes

1. Beller, G. A.; Bergman, S. R. *J. Nucl. Cardiol.* **2004**, *11*, 71.
2. Opie, L. H. In *Heart Disease: A Textbook of Cardiovascular Medicine*; Braunwald, Eugene, Ed., 6th ed.; W.B. Saunders: Philadelphia, 2001; p 443.
3. (a) Martarello, L.; Greenamyre, T.; Goodman, M. M. *J. Label. Compd. Radiopharm.* **1999**, *42*, 1039; (b) Charalambous, A.; Manger, T. J.; Kilbourn, M. R. *Nucl. Med. Biol.* **1995**, *22*, 65; (c) Charalambous, A.; Tluczek, L.; Frey, K. A.; Higgins, D. S.; Greeenmyre, T. J.; Kilbourn, M. R. *Nucl. Med. Biol.* **1995**, *22*, 491; (d) VanBrocklin, H. F.; Enas, J. D.; Hanrahan, S. M.; O'Neil, J. P. *J. Label. Compd. Radiopharm.* **1995**, *37*, 217; (e) Enas, J. D.; Hanrahan, S. M.; VanBrocklin, H. F. *J. Label. Compd. Radiopharm.* **1995**, *37*, 220.
4. Marshall, R. C.; Powers-Risius, P.; Reutters, B. W.; Taylor, S. C.; VanBrocklin, H. F.; Huesman, R. H.; Budinger, T. F. *J. Nucl. Med.* **2001**, *42*, 272.
5. (a) Esposti, M. D. *Biochim. et. Biophys. Acta* **1998**, *1364*, 222; (b) Nicolaou, K. C.; Pfefferkorn, J. A.; Schuller, F.; Roecker, A. J.; Cao, G.-Q.; Casida, J. E. *Chem. Biol.* **2000**, *7*, 979; (c) Lindell, S. D.; Ort, O.; Lummen, P.; Klein, R. *Bioorg. Med. Chem. Lett.* **2004**, *14*, 511.
6. Latli, B.; Wood, E.; Casida, J. E. *Chem. Res. Toxicol.* **1996**, *9*, 445.
7. Okun, J. G.; lumen, P.; Brandt, U. *J. Biol. Chem.* **1999**, *274*, 2625.
8. Wood, E.; Latli, B.; Casida, J. E. *Pest. Biochem. Physiol.* **1996**, *54*, 135.
9. Lamberth, C.; Hillesheim, E.; Bassand, D.; Schaub, F. *Pest. Manag. Sci.* **2000**, *56*, 94.
10. Drikhorn, B. A.; Graupner, P. R.; Liebeschuetz, J. W.; Yap, M. *ACS Symp. Series* **1998**, *686*, 273, Synthesis and Chemistry of Agrochemicals V.
11. Hirata, K.; Kawamura, Y.; Kudo, M.; Igarashi, H. *J. Pesticide Sci.* **1995**, *20*, 177.
12. Kirby, N. B.; Daeuble, J. F.; Davis, L. N.; Hannum, A. C.; Hellwig, K.; Lawler, L. K.; Partker, M. H.; Peczko, M. E. *Pest. Manag. Sci.* **2001**, *57*, 844.
13. (a) Hackler, R. E.; Suhr, R. G.; Sheets, J. J.; Hatton, C. J.; Johnson, P. L.; Davis, L. N.; Edie, R. G.; Kaster, S. V.; Jourdna, G. P., et al. *Special Publication—Royal Society of Chemistry* **1994**, *147*, 70, Advances in the Chemistry of Insect control III; (b) Haley, G.J.U.S. Patent 5270466, 1993.
14. Alkorta, I.; Rozas, I.; Elguero, J. *J. Fluor. Chem.* **2000**, *101*, 233.
15. Magata, Y.; Lang, L.; Kiesewetter, D. O.; Jagoda, E. M.; Channing, M. A.; Eckelman, W. C. *Nucl. Med. Biol.* **2000**, *27*, 163.
16. The procedure for determining the catalytic activity of submitochondrial particles or IC_{50} values was adapted from Satoh et al. (*Biochim. et. Biophys. Acta* **1996**, *1273*, 21–30). NADH-DB reductase activity was measured using a stirred cuvette in a spectrophotometer (Hewlett-Packard, Houston TX) at 37 °C, as the rate of NADH oxidation at 340 nm ($\varepsilon = 5.4$ mM$^{-1} \times$ cm^{-1}) for 120 s. The final volume of the reaction was 2.5 ml, containing 50 mM K_2HPO_4 (pH 7.4), 0.4 μM Antimycin A, and 2 mM KCN. The final SMP concentration was 45 μg/ml. The enzyme reaction was initiated by the addition of 100 μM decyl ubiquinone (DB) and 50 μM NADH. Inhibitors at varying concentrations were pre-incubated with the reaction mixture containing SMPs for 4 min prior to initiation of the reaction. The IC_{50} value was calculated using GraphPad Prism software (GraphPad, San Diego, CA).
17. Davis, S.; Weiss, M. J.; Wong, J. R.; Lampidis, T. J.; Chen, L. B. *J. Biol. Chem.* **1985**, *26*, 13844.
18. Zhanf, H.; Li, B.; Dai, M. *J. Pharm. Pharmacol.* **2003**, *55*, 505.
19. Piwnicaia-Worms, D.; Kronauge, J. F.; Chiu, M. L. *Circulation* **1990**, *82*, 1826.
20. Ott, H.; Denzer, M. *J. Org. Chem.* **1968**, *33*, 4263.
21. Singh, H.; Aggarwal, S. K.; Malhotra, N. *Tetrahedron* **1986**, *42*, 1139.
22. The identity as to whether this compound was a 1-methyl or 3-methyl quinazolinium iodide was not determined due to the low inhibition.
23. The ^{18}F is received from PETNET as a deposited sodium salt on a processed elutable column. It is eluted from the column using a mixture of K_2CO_3 and Kryptofix (K_{222}) dissolved in water and acetonitrile, respectively, into a vial containing the precursor dissolved in acetonitrile.